Multi-Objective Reliability and Resilience Assessment of Electrical Distribution Networks Using Optimized Adaptive Protection and Fault Management Strategies

Sunday Akano[1], Muniru Olajide Okelola[2]
[1,2]Department of Electronic and Electrical Engineering,
Ladoke Akintola University of Technology,
P.M.B, 4000, Ogbomoso, Nigeria.
Corresponding Email: abumbum1202@gmail.com
https://doi.org/10.56201/ijemt.vol.12.no10.2026.pg213.225

Abstract
Modern distribution feeders operate under changing demand, distributed generation, network reconfiguration, and increasingly demanding continuity-of-supply requirements. Protection systems must therefore do more than interrupt faults quickly: they must isolate damaged sections selectively and support the recovery of healthy loads. This article presents a multi-objective assessment framework that links adaptive overcurrent protection, fault management, customer reliability, and network resilience. The proposed application considers the IEEE 33-bus and IEEE 69-bus distribution networks under common fault and restoration conditions. Three alternatives are examined: conventional fixed-setting protection, adaptive relay-setting selection, and integrated adaptive protection with coordinated switching and restoration. Inverse-time relay characteristics and primary–backup coordination constraints are combined with the system average interruption frequency index, system average interruption duration index, annual energy not supplied, and a twelve-hour load-service resilience index. A hybrid particle swarm–grey wolf optimizer is proposed for identifying feasible trade-offs among clearing time, customer interruption, unserved energy, and restoration performance. For a transparent numerical comparison, the article uses stipulated scenario inputs rather than results from a completed feeder simulation. Within these scenarios, the IEEE 33-bus average clearing times are 0.64, 0.43, and 0.28 seconds for the three strategies. Corresponding interruption durations are 12.0, 8.3, and 5.7 hours per customer annually, while event resilience scores are 0.68, 0.81, and 0.90. The IEEE 69-bus resilience scores follow the same pattern at 0.62, 0.76, and 0.87. The comparisons illustrate potential benefits of coordinated decisions but do not independently verify the stated improvements. Practical application requires benchmark-data validation, short-circuit modelling, realistic device characteristics, secure communications, and feasible restoration paths. The framework provides a consistent technical basis for evaluating whether protection improvements translate into measurable customer-service benefits in active distribution networks. Particular attention is given to coordination security, correct interruption accounting, continuity for essential services, and the need to carefully test parameter uncertainty before practical deployment decisions.

Keywords: *Adaptive protection; Distribution reliability; Network resilience; Relay coordination; Multi-objective optimization; Fault management; Energy not supplied.*

1. Introduction

Electrical distribution networks now supply increasingly diverse consumers while also accommodating rooftop generation, storage, controllable demand, and remotely operated switching equipment. These developments create operating conditions that change over the course of a day and after contingencies. In such networks, a relay setting that is satisfactory for one feeder topology or generation pattern may be too slow, too sensitive, or insufficiently selective under another. A fault can then interrupt healthy sections even where alternative supply routes remain available. Uma et al. (2023) examined adaptive overcurrent coordination in the presence of distributed generation, and Elsadd et al. (2023) drew attention to coordination difficulties during reconfiguration and fault repair.

The effects of these interruptions are commonly quantified using the system average interruption frequency index (SAIFI), the system average interruption duration index (SAIDI), and energy not supplied (ENS). SAIFI records sustained interruptions per customer, SAIDI measures the time customers remain without service, and ENS captures the associated energy deficit. Yet the ability to cope with a major disturbance requires a further perspective: how much load remains energized, how quickly essential services return, and whether recovery actions are physically feasible. Resilience analysis therefore complements conventional reliability studies by following network service throughout a specified recovery interval. Tang et al. (2024) emphasize the connected roles of fault location, response, and restoration in resilient distribution operation.

Protection and restoration are increasingly examined as interacting decisions rather than unrelated utility activities. Chen et al. (2024) incorporated component repair and restoration scheduling into a multi-period network model. Beiranvandi et al. (2024) considered restoration after widespread disturbance, while Pereira et al. (2025) investigated the joint allocation of distributed generation and protection devices in a multi-objective setting. These investigations suggest that the value of a protection upgrade should be judged not only by relay operating time, but also by the extent of selective isolation and the amount of customer demand restored. At the same time, no protection algorithm can restore a broken feeder without a safe supply path or completed repair.

This paper organizes those relationships into a common comparison of three protection and fault-management strategies. Each strategy is assigned the same feeder equipment, switching infrastructure, and disturbance set. The comparison asks whether adapting relay settings, and subsequently coordinating them with isolation and restoration decisions, can improve annual reliability and disturbance-event resilience without compromising protection coordination. A mathematical framework and worked scenario dataset are provided to make the expected calculations and reporting requirements explicit.

The study pursues five objectives: to formulate practical primary–backup relay constraints; to connect adaptive protection with selective fault isolation; to compare customer-oriented annual reliability indices; to evaluate an event-based energy-service resilience measure; and to specify verification tests covering distributed generation, communication delays, and uncertain recovery conditions. Its central research question is whether integrated protection and fault management can offer a demonstrable advantage over adaptive relay-setting selection alone when all options operate with equivalent resources.

2. Related Works

Uma et al. (2023) applied a radial-basis-function neural network to adaptive overcurrent protection in a distribution system containing distributed generation. Their work underscores the usefulness of recognizing changing network states before selecting relay settings. Elsadd

et al. (2023) examined relay coordination without continuous communication during periods of network repair and reconfiguration. Both studies support the practical use of setting groups that remain feasible across admissible feeder configurations. The present framework extends that discussion to customer outage durations and post-event service restoration.

Tang et al. (2024) surveyed strategies for enhancing distribution resilience, discussing the sequence from disturbance detection to system recovery. A central implication is that faster fault detection does not automatically mean a proportional improvement in service restoration. Beiranvandi et al. (2024) addressed the restoration of multi-area active networks after severe disruption, highlighting resource allocation and network cooperation. Chen et al. (2024) combined rapid restoration with repair scheduling in a multi-period formulation. These studies show why a resilience result must specify its recovery horizon, the resources available, and the load actually supplied during the event.

A broader optimization perspective is provided by Pereira et al. (2025), who considered distributed-generation placement together with protection and control devices while accounting for economic and energy-related objectives. Their formulation reinforces the need to define competing performance criteria and normalize them carefully. Kuriakose et al. (2025) reviewed the opportunities and limitations of optimization methods used for relay coordination. Liu et al. (2025) linked dispatch decisions, repair activities, and priority-load restoration. Building on these insights, the present study examines coordinated protection and recovery without granting one strategy additional installed network assets.

Adaptive protection also introduces implementation risks. Ghotbi-Maleki et al. (2025) discussed cyber-attacks targeting relay settings and the need for dependable safeguards. Mohamed et al. (2026) compared alternative optimizers for relay coordination in distribution systems containing distributed generation, emphasizing that an algorithm must be evaluated through its feasible settings rather than its name. Ji et al. (2026) investigated fault repair and network reconfiguration under uncertainty. Together, these contributions motivate a formulation that treats protection security, restoration feasibility, and uncertainty testing as essential elements of performance evaluation.

2.1 Research Gap and Position of the Study

An opportunity remains for a single, clearly specified evaluation procedure that connects protection coordination with both annual customer reliability and the time-dependent recovery of load after an exceptional event. These measures are related, but they have different accounting periods and physical meanings. The approach developed here preserves that distinction, compares three decisions architectures under equal resources, and establishes explicit safeguards against interpreting a shorter relay operating time as automatic evidence of lower SAIDI or higher resilience.

3. Methodology

3.1 Networks, Data Inputs and Comparative Schemes

The proposed benchmark networks are the IEEE 33-bus and IEEE 69-bus radial feeders, both operated at a nominal voltage of 12.66 kV. Their validated line, load, and topology datasets are required for a future implementation. The study framework considers distributed-generation penetration levels of 0%, 20%, 40%, and 60% and permits grid-connected operation or technically admissible islanded sections. Fault categories include single-line-to-ground, line-to-line, and three-phase faults, with a scenario fault-resistance range of 0.1–10 Ω. Annual reliability modelling requires branch failure and repair distributions; a separate twelve-hour event examines load recovery after a multi-section disturbance.

Scheme A uses conventional overcurrent relays with fixed settings and standard restoration

procedures. Scheme B permits the selection of prevalidated relay-setting groups as operating conditions change, while retaining the same switching and restoration equipment. Scheme C coordinates those adaptive settings with sectionalizing, restoration dispatch, and the use of installed distributed generation or storage. Hardware inventories and disturbance assumptions remain equivalent across the schemes. Communication and decision delays must be included where applicable, and primary–backup relay assignments must be reconsidered whenever the network topology changes.

Table 1. Proposed benchmark assumptions (for prospective verification).

Element	IEEE 33-bus	IEEE 69-bus
Nominal feeder voltage	12.66 kV	12.66 kV
DG penetration cases	0, 20, 40, 60%	0, 20, 40, 60%
Fault resistance range	0.1–10 Ω	0.1–10 Ω
Protection CTI minimum	0.20 s	0.20 s
Resilience recovery horizon	12 h	12 h
Fault scenario weights	To be calibrated	To be calibrated
Annual failure/repair data	To be collected	To be collected

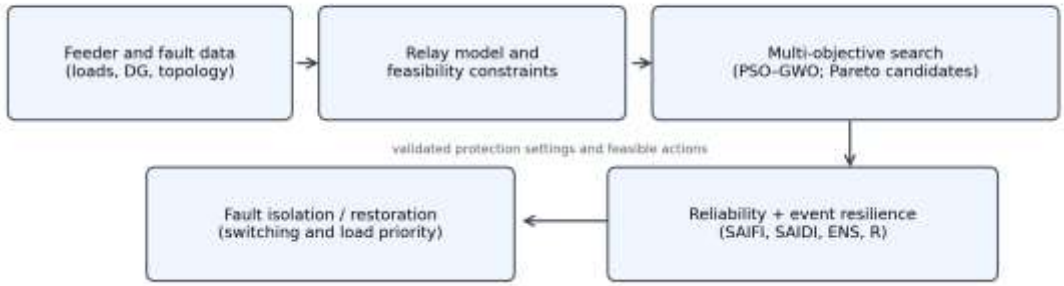


Figure 1. Proposed integrated protection–fault management–reliability assessment workflow (methodological schematic).

3.2 Fault Analysis and Relay Coordination Model

Fault studies begin with the sequence-network model and an explicit description of the fault-current contributions from distributed generators. For a balanced three-phase fault, the Thevenin expression in Equation (1) provides a preliminary estimate. Final current magnitudes at each relay location require short-circuit calculations for the relevant fault type, network topology, grounding configuration, and generator operating condition:

$I_{3\varphi} \approx |V_{pre}| / |Z_{th} + Z_f|$ (1)

Here Vpre denotes prefault voltage, Zth the Thevenin impedance, and Zf the fault impedance. This approximation does not replace unbalanced-fault calculations or the control-limited current response of inverter-based generation. Relay operation is modelled with the standard inverse-time characteristic in Equation (2):

$t_r = [0.14 \times TMS_r] / [(I_r / I_{p,r})^{0.02} - 1], \quad I_r > I_{p,r}$ (2)

The relay operating time tr depends on its time multiplier TMSr, the measured current Ir, and the pickup threshold Ip,r. For each applicable fault scenario s, a backup device b should operate only after its assigned primary relay p, subject to the minimum coordination interval in Equation (3):

$t_{b,s} - t_{p,s} \geq CTI_{min}, \quad CTI_{min} = 0.20\ s$ (illustrative) (3)

This protection constraint is meaningful only when the primary and backup devices detect the fault with adequate sensitivity. Breaker operating delays, pickup limits, directional

requirements, and thermal withstand limits must be incorporated consistently. Feasible settings must also respect time-multiplier bounds and maximum load currents. Coordination-violation percentages are evaluated only for fault cases with an identified, technically valid primary–backup relay pair.

3.3 Reliability and Resilience Measures

Annual customer reliability is described at load point j by interruption frequency λj, annual interruption duration Uj, number of customers Nj, and reference demand Pj. Summing over all load points gives the standard indices in Equations (4)–(6):

$SAIFI = \Sigma j(\lambda j\ Nj) / \Sigma j\ Nj$ [interruptions/customer/year] (4)

$SAIDI = \Sigma j(Uj\ Nj) / \Sigma j\ Nj$ [hours/customer/year] (5)

$ENSannual = \Sigma j(Pj\ Uj) / 1000$ [MWh/year] (6)

Annual indices require a consistent accounting of component failures, customer interruptions, and the duration of repair or restoration. Momentary disturbances should be treated according to the adopted utility reporting convention and not added indiscriminately to sustained interruptions. For a distinct event with demand D(t), delivered power S(t), and an observation interval T, unserved energy and service resilience are calculated using Equations (7) and (8):

$ENSE = \int_0^T \max[D(t) - S(t),0]\ dt$ (7)

$R = 1 - ENSE / \int_0^T D(t)\ dt = \int_0^T \min[S(t),D(t)]\ dt / \int_0^T D(t)\ dt$ (8)

When served demand does not exceed the required demand, R falls between zero and one and represents the share of the requested energy actually delivered during the event. It should not be interpreted as a universal probability of network survival. Annual ENS and the energy deficit of one disturbance are reported separately. The restoration model may prioritize critical facilities explicitly, while SAIFI and SAIDI continue to follow their customer-based definitions.

3.4 Multi-Objective Formulation and Solution Procedure

The optimization decisions comprise relay pickup currents, time-multiplier settings, operating-state setting groups, permitted switch positions, and restoration dispatch. Solutions must satisfy protection coordination, fault sensitivity, voltage and thermal limits, available generation, storage constraints, restoration crew availability, and feasible network topology. Four objectives are normalized to allow comparison across unlike units:

$\min F(x) = [Tclear(x)/Tref, SAIDI(x)/Sref, ENSannual(x)/Eref, 1 - R(x)]$ (9)

A weighted objective can provide an initial search direction, but the final engineering trade-offs should be evaluated using Pareto dominance and an ε-constraint check. For scenario screening, one possible aggregate is $J = 0.20F1 + 0.25F2 + 0.25F3 + 0.30F4$, subject to rejection or penalty of infeasible coordination solutions. A hybrid particle swarm–grey wolf optimizer (PSO–GWO) is proposed to explore setting and restoration choices, with feasibility checks applied before scoring each candidate. Comparative studies should include conventional optimization baselines, repeated random seeds, and transparent reporting of constraint violations; a hybrid algorithm is not intrinsically superior without such evidence.

The evaluation is organized into six stages. Feeder power flow and short-circuit cases are first validated. Primary and backup relays are then assigned for each permitted topology. The three protection strategies are evaluated against the same fault set, followed by annual failure-and-repair scenarios for reliability assessment. A separate twelve-hour contingency is used to examine isolation, switching, and recovery of load. Finally, distributed-generation sensitivity, communication delays, fallback operation, and parameter uncertainty are tested. A reproducible study should disclose the software version, component assumptions, network data, random seeds, and number of scenarios.

4. Results and Discussion

The following numerical comparisons are scenario-based examples built from the defined assumptions; they are not outputs of an executed benchmark short-circuit, Monte Carlo reliability, or restoration-optimization study. Their purpose is to illustrate how the performance measures fit together and to identify the evidence required for a subsequent computational validation. The reported values and plotted relationships are interpreted consistently within that scope.

4.1 Fault-Clearance Performance and Selectivity

Table 2. Protection-coordination performance for the defined comparison scenarios.

Index	33-bus: A / B / C	69-bus: A / B / C
Mean clearance time (s)	0.64 / 0.43 / 0.28	0.79 / 0.52 / 0.34
CTI violations (%)	16 / 6 / 1	20 / 8 / 2
Selective isolation success (%)	83 / 94 / 99	80 / 92 / 98

In the 33-bus scenario, mean fault clearance changes from 0.64 s under Scheme A to 0.43 s under Scheme B and 0.28 s under Scheme C. These values correspond to relative decreases of 32.8% and 56.3% compared with fixed protection. On the 69-bus feeder, the change from 0.79 s to 0.34 s amounts to 57.0%. The comparison highlights a plausible benefit of adapting settings to network conditions while preserving suitable backup delays. Because means can conceal slow-clearing faults, a completed protection study should also present worst-case clearance times and the distribution of results across fault locations and operating conditions.

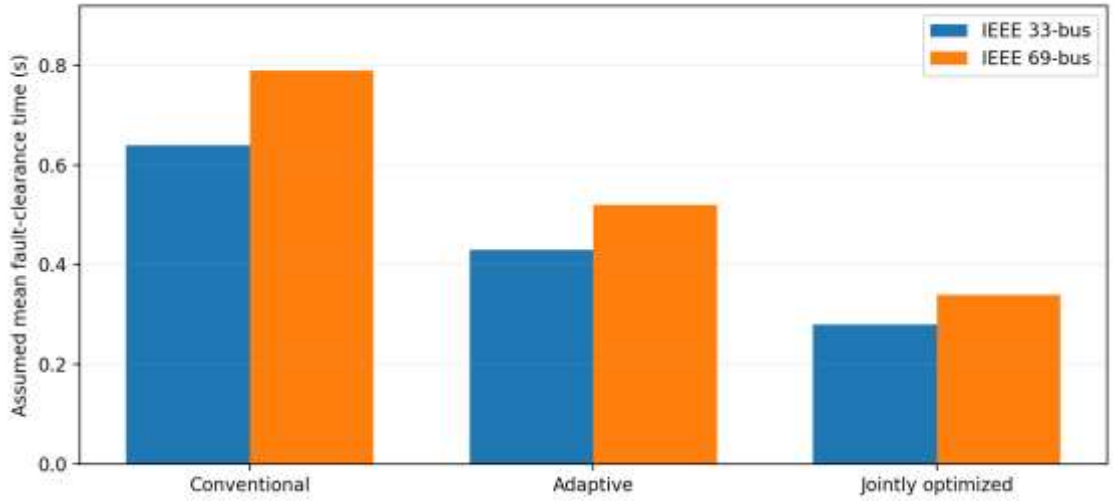


Figure 2. Mean fault-clearance times for the three strategies in the defined scenarios.

Coordination-violation rates follow the same descending pattern, reaching 1% on the 33-bus feeder and 2% on the 69-bus feeder for Scheme C. Importantly, any credible coordination violation requires investigation before field deployment; a low average percentage does not establish protection security. Selective-isolation success is also reported independently because unwanted operations can arise from inadequate fault sensitivity, incorrect directional decisions, or blind zones even where time grading appears satisfactory. A full validation should therefore identify the specific cases that violate limits and report primary operation, backup operation, and false-trip frequencies.

4.2 Customer-Oriented Reliability Indices

Table 3. Annual reliability indices under common failure and restoration scenarios.

Network and metric	Conventional A	Adaptive B	Joint C
33-bus SAIFI (interruptions/cust·yr)	1.65	1.35	1.15
33-bus SAIDI (h/cust·yr)	12.0	8.3	5.7
33-bus annual ENS (MWh)	39	28	19
69-bus SAIFI (interruptions/cust·yr)	1.95	1.55	1.32
69-bus SAIDI (h/cust·yr)	15.0	10.8	7.6
69-bus annual ENS (MWh)	54	38	27

For the 33-bus example, SAIFI decreases across Schemes A, B, and C from 1.65 to 1.35 and 1.15 interruptions per customer-year. SAIDI follows the same ordering at 12.0, 8.3, and 5.7 hours per customer-year, giving a 52.5% difference between the fixed and joint strategies. The corresponding 69-bus duration values are 15.0 and 7.6 hours per customer-year, a 49.3% difference. These changes would be attributable to better fault-section isolation and successful restoration under the scenario assumptions, not merely to reductions of a few tenths of a second in relay operating time. Measured utility records or a validated interruption model would be required to establish them empirically.

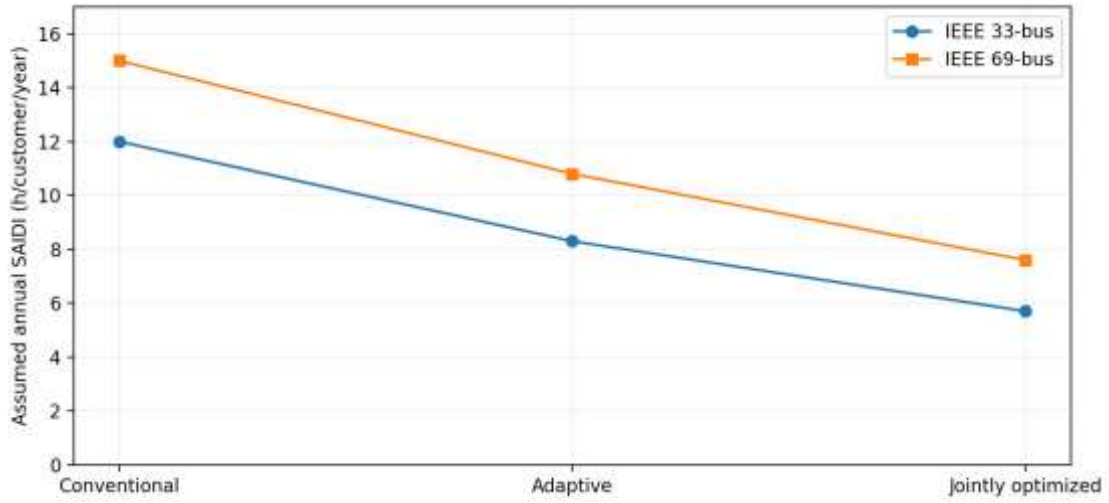


Figure 3. Annual customer interruption duration for the three strategies.

The 33-bus annual energy deficit decreases from 39 to 19 MWh between Schemes A and C, corresponding to a 51.3% difference. In the 69-bus example, annual ENS changes from 54 to 27 MWh, a 50.0% difference. ENS gives larger weight to interruptions affecting substantial loads, so it complements customer-count indices in comparing alternative restoration choices. Network-level averages should nevertheless be accompanied by load-point results to ensure that service at hospitals, businesses, or other essential facilities is not worsened while aggregate indicators improve.

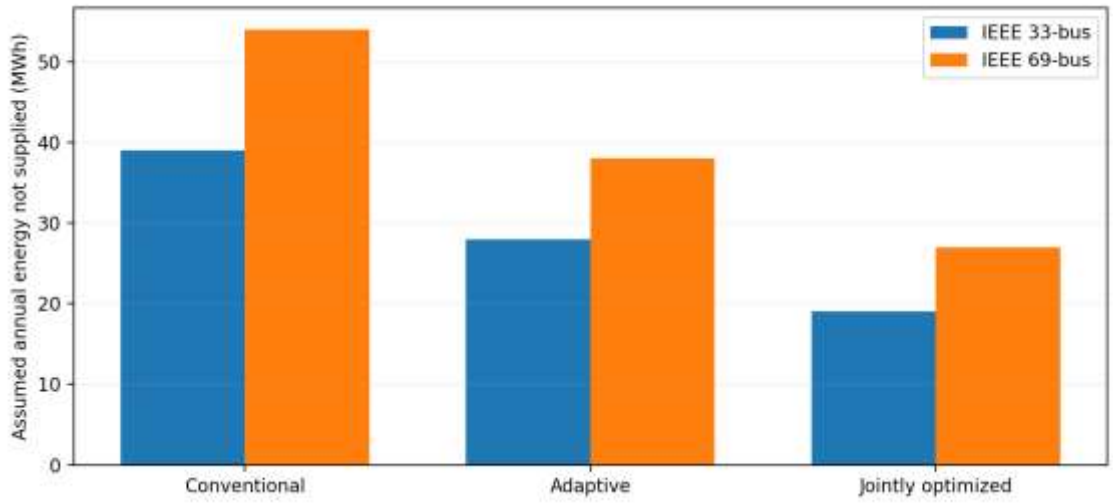


Figure 4. Annual energy not supplied for the three protection and restoration scenarios.

4.3 Event-Level Resilience Under a Twelve-Hour Recovery Horizon

For the twelve-hour event, a fixed reference demand of 3.0 MW is specified for the 33-bus scenario and 3.8 MW for the 69-bus scenario. The corresponding demanded energies are 36.0 and 45.6 MWh. The event-based resilience values in Table 4 are related directly to event ENS through ENSE = (1 − R) Eref. Using a common reference demand within each feeder prevents differences in load assumptions from being mistaken for changes in protection effectiveness. These event deficits must remain distinct from the annual ENS estimates in

Table 3.

Table 4. Event-service resilience and energy deficits over twelve hours.

Network	Scheme A	Scheme B	Scheme C
33-bus R (fraction)	0.68	0.81	0.90
33-bus event ENS (MWh)	11.52	6.84	3.60
69-bus R (fraction)	0.62	0.76	0.87
69-bus event ENS (MWh)	17.33	10.94	5.93

Under the stipulated recovery trajectories, Scheme C supplies 90% of the required energy on the 33-bus system, compared with 68% under Scheme A. This implies 3.60 MWh of unserved event demand for Scheme C and 11.52 MWh for Scheme A. On the 69-bus system, the corresponding scenario deficits are 5.93 and 17.33 MWh. These system-wide indices should be supplemented with time-to-restore metrics for critical customers. A high overall service fraction does not guarantee that a hospital, water pumping station, or communications facility was restored within an acceptable period.

The 33-bus load-service trajectories in Figure 5 are parameterized by $S(t)/D = \beta + (1 - \beta)(t/12)^{\alpha}$, where $\alpha = (1 - \beta)/(R - \beta) - 1$. This construction ensures that each curve integrates to its stated twelve-hour resilience index. Initial served-load fractions are set at 0.18, 0.36, and 0.50 for Schemes A, B, and C, respectively. The curves therefore demonstrate the index calculation; they are not simulated switching operations or observed feeder restoration histories.

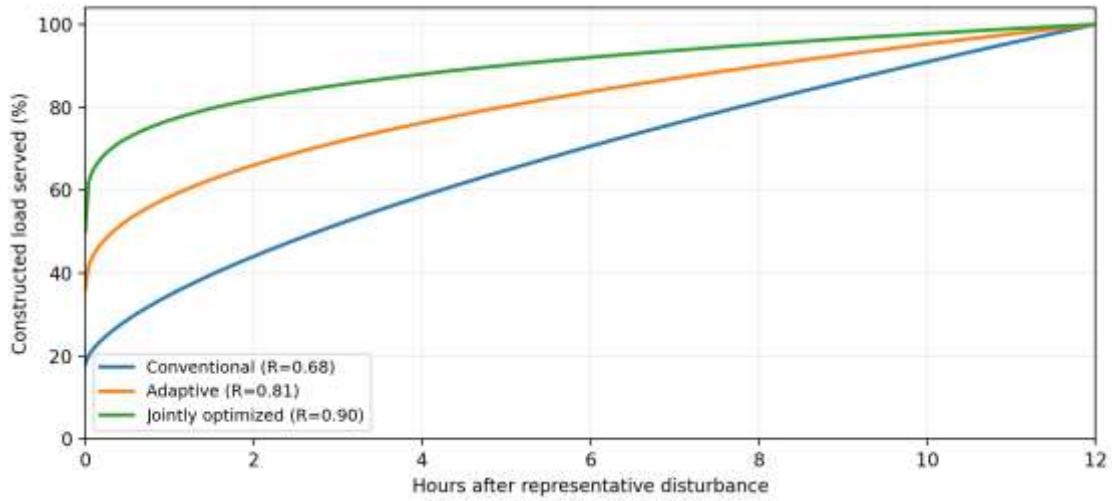


Figure 5. Load-service recovery curves consistent with the event resilience scores.

4.4 Sensitivity to Distributed Generation and Protection Communication

Table 5. Protection-coordination sensitivity to distributed-generation penetration.

DG penetration	A fixed (%)	B adaptive (%)	C joint (%)
0%	4	2	1
20%	8	3	1
40%	16	6	2
60%	24	11	4

In the 33-bus sensitivity example, the fixed-setting scheme's coordination-violation rate increases from 4% at zero distributed generation to 24% at 60% penetration. The corresponding end-point values for adaptive and joint operation are 11% and 4%. This pattern expresses the expected challenge posed by redistribution and limitation of fault currents as distributed resources change operating states. Penetration percentage alone, however, cannot determine relay behaviour. A validated analysis must vary generator technology and siting, grounding, impedance, inverter controls, and fault direction separately.

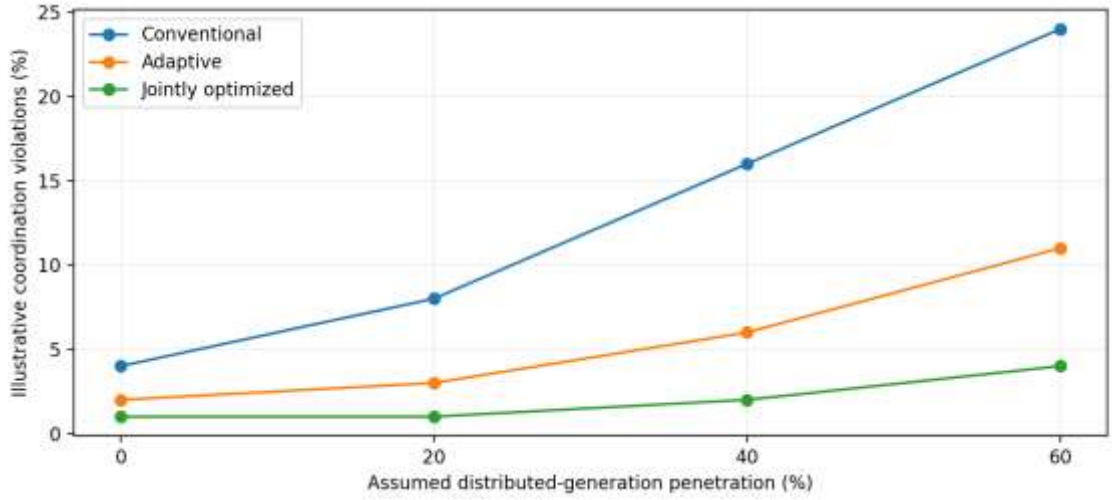


Figure 6. Coordination-violation sensitivity across distributed-generation levels.

Table 6. Communication, uncertainty, and implementation tests required for verification.

Test	Outcome that must be recorded
50 ms / 150 ms message delay	Clearance-time distribution and CTI feasibility
Complete communication outage	Secure fallback setting and fault coverage
DG output / fault resistance uncertainty	Worst-case relay sensitivity, missed trips
Switch or crew unavailability	Feasible restoration and event ENS
10–30 stochastic seeds per optimizer	Variability, confidence interval, convergence

Adaptive protection introduces delays associated with measurement filtering, local computation, communication, and breaker interruption. These contributions should be measured or modelled explicitly rather than treated as instantaneous. In the event of communications loss, a prevalidated fallback setting should preserve dependable fault clearing, although it may increase the interruption period. Ghotbi-Maleki et al. (2025) show why setting-change integrity and secure fallback are relevant to active-network protection. Robustness should also be tested over alternative objective weights to ensure that improved service restoration does not conceal unsafe relay-coordination choices.

4.5 Cross-Objective Interpretation and Practical Limitations

The scenario results should be read as a structured examination of competing engineering objectives, not as independent measurements. In an actual feeder model, reducing the pickup current may improve sensitivity but increase unwanted operations; increasing it may protect against nuisance trips at the expense of difficult faults. Likewise, aggressive feeder switching may raise the served-load fraction but violate thermal, voltage, or operational limits. The usefulness of a multi-objective method lies in making these trade-offs visible while rejecting technically infeasible options. Reliability and resilience also require different evidence. Annual SAIFI, SAIDI, and ENS depend on failure rates, repairs, and customer interruption records across many contingencies, whereas the twelve-hour resilience index describes one bounded recovery event. Neither result can be inferred directly from the other. A future study should replicate benchmark network behaviour, compare independent optimization methods, report results over repeated trials, quantify uncertainty, and calibrate the model with feeder-specific information where available.

5. Conclusions

The article has presented a unified procedure for investigating whether optimized adaptive protection and coordinated fault management can improve the reliability and resilience of electrical distribution networks. Two standard feeder benchmarks—the IEEE 33-bus and IEEE 69-bus networks—provide a common foundation for three alternatives: conventional fixed settings, adaptive protection, and integrated adaptive protection with fault isolation and restoration. The comparison is designed so that changes in outcomes arise from the decision strategy rather than an unequal allocation of network hardware.

The proposed methodology links short-circuit analysis, inverse-time relay operation, pickup sensitivity, and primary–backup timing to indices that matter directly to electricity consumers. Annual SAIFI, SAIDI, and ENS describe recurring service interruptions; a separate load-service integral describes recovery during an individual prolonged event. This separation is essential. Faster protection may reduce fault exposure, but an improvement in customer interruption or resilience additionally depends on isolation boundaries, restoration

paths, distributed energy availability, and the time needed to repair damaged equipment.
The specified 33-bus scenarios move from 0.64 s to 0.28 s in mean clearance time, from 12.0 to 5.7 h/customer-year in SAIDI, and from 39 to 19 MWh/year in annual ENS between Schemes A and C. The twelve-hour resilience score increases from 0.68 to 0.90. On the 69-bus feeder, the corresponding scenario values show SAIDI changing from 15.0 to 7.6 h/customer-year and resilience from 0.62 to 0.87. These are scenario-derived comparisons based on stipulated inputs, not verified performance improvements from an executed electrical-network simulation. Before the approach can support field recommendations or empirical publication claims, it must be evaluated with traceable line and demand data, credible inverter fault-current models, detailed protective-device settings, component failure distributions, and time-dependent restoration calculations. Multiple fault locations, resistance values, generation conditions, communication failures, and optimization runs should be included. Every admissible relay setting must meet mandatory sensitivity and primary–backup coordination safeguards, even if a less conservative setting would otherwise produce a lower aggregate objective value. The principal conclusion is that protection performance should be linked explicitly to customer reliability and disturbance recovery, without treating the three as interchangeable. Future validation should establish whether adaptive settings improve secure fault selection, whether coordinated isolation reduces the duration of sustained outages, and whether the same network resources can maintain a larger share of electrical service through a serious contingency. Extension to a documented Nigerian 33-kV feeder would make the framework directly relevant to local distribution conditions.

6. Contribution to Knowledge

The first contribution is a common methodological basis for comparing three protection and fault-management approaches. Fixed relay settings, adaptive setting groups, and joint protection–restoration decisions are evaluated under equivalent network assets, disturbances, and accounting periods. This makes the interpretation of future performance differences more defensible than comparisons involving dissimilar feeder investments.
Second, the formulation connects the feasibility of relay coordination to the ability to restore electricity supply. Pickup thresholds, time multiplier settings, backup delays, directional requirements, network switching, and dispatch decisions are treated within a coherent set of constraints. A shorter relay operating time is not counted as restored customer service unless a safe supply route or completed component repair actually makes that service available.
Third, the study introduces a multi-objective assessment that retains the separate meanings of mean fault-clearance time, annual interruption duration, annual unserved energy, and event resilience loss. Pareto analysis enables explicit discussion of conflicts between these objectives. Protection and network operating constraints remain binding, preventing an optimization method from endorsing technically unsafe solutions on the strength of a favorable aggregate score. Fourth, the analysis distinguishes reliability from resilience through clear time horizons and units. SAIFI, SAIDI, and annual ENS describe recurrent component outages and repairs; the resilience index quantifies the fraction of demand served over a specified disturbance interval. Maintaining these distinct measures avoids comparing customer-year quantities directly with the recovery of one event.
Fifth, the article supplies a self-consistent set of scenario calculations that links resilience scores with twelve-hour energy deficits and associated load-service curves. The arithmetic relationship between required energy, delivered energy, and event ENS remains explicit, providing a transparent basis for later replication with computed or measured time series.
Sixth, the proposed verification protocol covers distributed-generation penetration, fault resistance, communications latency and loss, secure fallback settings, restoration-resource

constraints, and stochastic optimizer variability. These elements provide a practical foundation for moving from the present analytical comparison to fully reproducible benchmark simulations and, subsequently, evaluation on a documented Nigerian distribution feeder. Any claim of technical novelty or superior protection performance should ultimately rest on those validated tests.

7. References

Beiranvandi, H., Samanfar, A., Doostizadeh, M., & Saki, R. (2024). A resilience-oriented restoration framework for multi-area active distribution network following a disaster. IET Renewable Power Generation, 18, 3810–3824. https://doi.org/10.1049/rpg2.13042

Chen, L., Jiang, Y., Deng, X., Zheng, S., Chen, H., & Islam, M. R. (2024). A multi-period restoration approach for resilience increase of active distribution networks by considering fault rapid recovery and component repair. International Journal of Electrical Power & Energy Systems, 161, 110181. https://doi.org/10.1016/j.ijepes.2024.110181

Elsadd, M. A., Zobaa, A. F., Khattab, H. A., Abd El Aziz, A. M., & Fetouh, T. (2023). Communicationless overcurrent relays coordination for active distribution network considering fault repairing periods. Energies, 16(23), 7862. https://doi.org/10.3390/en16237862

Ghotbi-Maleki, M., Azzouz, M. A., & Sanaye-Pasand, M. (2025). Resilience enhancement of adaptive overcurrent protection for active distribution networks against relay-setting cyber-attacks. IEEE Transactions on Industrial Informatics, 21(11), 9034–9044. https://doi.org/10.1109/TII.2025.3594016

Ji, X., Han, H., Zhang, H., Si, C., Li, M., & Zhang, Z. (2026). A two-tier distribution robust distribution network resilience enhancement strategy accounting for fault repair and islanding fusion network reconfiguration. Scientific Reports, 16, Article 21500. https://doi.org/10.1038/s41598-026-51654-0

Kuriakose, A., Balamurugan, S., & Lekshmi, R. R. (2025). Relay coordination in resilient and sustainable power systems: Review on optimization techniques and future directions. International Journal of Electrical and Electronic Engineering & Telecommunications, 14(4), 199–212. https://doi.org/10.18178/ijeetc.14.4.199-212

Liu, W., Chen, K., Cheng, R., Yi, Y., Lu, H., & Zhang, Y. (2025). A coordinated strategy of flexible dispatch and fault repair for active distribution networks towards resilience enhancement. Electric Power Construction, 46(11), 10–23. https://doi.org/10.12204/j.issn.1000-7229.2025.11.002

Mohamed, R. E., Saleh, S. M., & Ahmad, A. G. (2026). Comparative optimization of overcurrent relay coordination in DG-integrated distribution networks: Water cycle algorithm versus genetic algorithm and big bang–big crunch. Scientific Reports, 16, Article 10529. https://doi.org/10.1038/s41598-026-43242-z

Pereira, K., Home-Ortiz, J. M., & Carreño Franco, E. M. (2025). A multi-objective optimization approach for integrated allocation of distributed generation and protection devices in distribution systems. IEEE Access, 13, 84139–84152. https://doi.org/10.1109/ACCESS.2025.3569431

Tang, L., Han, Y., Zalhaf, A. S., Zhou, S., Yang, P., Wang, C., & Huang, T. (2024). Resilience enhancement of active distribution networks under extreme disaster scenarios: A comprehensive overview of fault location strategies. Renewable and Sustainable Energy Reviews, 189, 113898. https://doi.org/10.1016/j.rser.2023.113898

Uma, U. U., Nmadu, D., Ugwuanyi, N., Ogah, O. E., Eli-Chukwu, N., Eheduru, M., & Ekwue, A. (2023). Adaptive overcurrent protection scheme coordination in presence of distributed generation using radial basis neural network. Protection and Control of Modern Power Systems, 8, Article 63. https://doi.org/10.1186/s41601-023-00336-4